Scientific Research Journal,
Vol 22, No 2 (2025) 83-97
https://doi.org/10.24191/srj.v22i2.23000

Effect of Deposition Temperature on The Structural and Crystallinity Properties of Self-Catalyzed Growth Indium Tin Oxide (ITO) Thin Film Using CVD Technique

Mardhiah Mohd Yunus, Azianty Saroni*

Faculty of Applied Sciences, Universiti Teknologi MARA Cawangan Pahang Kampus Jengka, 26400 Bandar Tun Abdul Razak Jengka Pahang, Malaysia

**Corresponding Author's E-mail:aziantysaroni@uitm.edu.my*

Received: 28 February 2025
Accepted: 29 April 2025
Online First: 01 September 2025

ABSTRACT

Indium Tin Oxide (ITO) is one of the electronic materials that is widely used as a transparent conductor in optoelectronic device applications. The growth techniques of ITO are crucial in order to grow the best structure of ITO for the better performance application. The main objective of this study to investigate the effect of deposition temperature (1000 °C, 1100 °C, and 1200 °C) on their structural and crystallinity properties of self-catalyzed ITO thin film synthesized using chemical vapor deposition (CVD) technique. The ITO thin films were deposited onto silicon substrates using a tube furnace via the CVD technique, utilizing a precursor mixture of indium(III) oxide (In_2O_3) and tin(IV) oxide (SnO_2), with argon gas used as the carrier. Scanning Electron Microscopy (SEM) showed that thin film at 1100 °C exhibited well-defined shapes, minimal aggregation, and an average diameter of 0.46 µm, making it the optimal temperature for synthesizing high-quality ITO thin film. Energy-dispersive X-ray (EDX) analysis confirmed the homogeneous distribution of indium, tin, and oxygen at this temperature, with the highest compositional homogeneity of 56.46%. Moreover, XRD pattern confirms the presence of peak at $2\theta = 31.1°$ corresponds to the (320) plane of cubic indium tin oxide ($In_2Sn_2O_7$) across all samples. Results show that as the deposition temperature increased, structures with well-defined shapes were formed, and the crystallinity was enhanced. The crystallite size increased from 35.21 nm to 103.05 nm as at 1000 °C and 1200 °C, respectively with

Copyright© 2020 UiTM Press.
This is an open access article
under the CC BY-NC-ND license

a corresponding decrease in lattice strain in the structure. These findings demonstrate how crucial the deposition temperature in determining the ideal structural properties of ITO thin film for application in particular optoelectronic devices.

Keywords: Indium Tin Oxide; Self-catalyzed Growth; Deposition Temperature; Structural Properties; Chemical Vapor Deposition

INTRODUCTION

Indium tin oxide (ITO) are made up of the composition of indium, tin, and oxygen [1]. These structures have different forms, including nanoparticles and nanowires [2]. ITO thin films are often synthesized using various techniques such as physical vapor deposition [3], chemical vapor deposition (CVD) [4], and sol-gel [5]. Tin-doped indium oxide (ITO) has been recognized as one of the most significant transparent conducting oxide (TCO) materials and commonly used in the application of optoelectronic devices such as light-emitting diodes (LED), solar cells, flat panel displays, and sensors [6]. Gold (Au) is one of the most often employed catalysts for the growth of ITO [7,8]. One disadvantage of employing a metal catalyst is that it may react with the target materials as they are growing, resulting in contamination and impurities.

Self-catalyzed growth is one of the methods in which ITO thin film grow naturally without the need of external catalysts. This growth process is commonly achieved by the vapor-phase deposition approach known as chemical vapor deposition. The technique involves the substrate's intrinsic features, catalyzing the creation of a catalyst and, hence, the formation of an ITO thin film [4,9]. In other word, the material to be grown as thin film itself acts as a catalyst. Self-catalyzed growth has several advantages, including simplicity, less contamination caused by external catalyst materials, and greater control over the growth process [4].

In order to grow the best ITO thin film, a lot of parameters need to be taken for consideration such as RF-power sputtering [6], temperature and pressure [10]. The deposition temperature has a considerable impact on the growth of ITO in terms of their structural properties. In general,

greater deposition temperatures stimulate the development of crystalline phases and increase the crystallinity of the deposited material. At higher deposition temperatures, the formation of greater crystallites with better crystallinity, resulting in increased electrical conductivity and optical transparency [11]. In appearance, higher temperatures could encourage the growth of larger grains [12]. As the grain size increased, key parameters influencing the electrical properties of the thin films, such as composition, surface roughness, thickness, and carrier concentration, are affected [13].

This study aims to explore the effect of deposition temperature on the self-catalyzed growth of ITO thin films to optimize structural and crystallinity properties. The morphology, structure, and composition of the formed ITO are analyzed using SEM and XRD. Understanding the influence of deposition temperature is essential for optimizing the properties of ITO thin films for high-performance optoelectronic applications, such as transparent electrodes and photodetectors.

EXPERIMENTAL METHODOLOGY

Sample preparation procedure

Indium (III) oxide (99.99% trace metal base) and Tin (IV) oxide (≥ 99.99% trace metal basis) were the chemicals used for the growth of crystalline ITO thin film. The method used was Chemical Vapor Deposition (CVD) on p-type Silicon, Si (111) substrate. In this study, sample preparation was done in a tube furnace. Indium oxide (In_2O_3) and tin oxide (SnO_2) powders were mechanically mixed at a weight ratio of 1:1. The mixture was transferred to an alumina boat, which was subsequently positioned in the hot zone of a horizontal tube furnace. To cover the alumina boat, a silicon (111) substrate was cleaned using a standard RCA I and RCA II procedure [14]. Initially the substrate was rinsed with deionized water before being immersed in a solution of H_2O, H_2O_2, and HCl in a 6:1:1 ratio for five minutes which is effective in removing metal ions and inorganic contaminants. The Si substrate was then rinsed with deionized water and immersed for five minutes in a solution of H_2O, H_2O_2, and NH_4OH in a 5:1:1 ratio targeting the removal of organic residues and particles. Subsequently, it was rinsed with deionized water before being immersed for five minutes

in a 10:1 solution of H_2O and HF, followed by a final rinse with deionized water to remove native oxide (SiO_2) from silicon substrates. A vacuum pump was adjusted to lower the pressure to approximately ~ 2×10^{-2} Torr and maintain it for about 10 minutes. Prior to the deposition, the tube furnace was adjusted to 1000 °C with a heating rate of 60 °C/minute, with argon (Ar) gas introduced. The pressure was set to 3 Torr and maintained for 70 minutes for the deposition. After deposition, the furnace was cooled to room temperature, and the samples were collected for analysis. The experiment was repeated with deposition temperatures of 1100 and 1200 °C to study the effects of varying temperature.

Sample characterization

Scanning Electron Microscopy (SEM, Tescan Vega 3) was used to analyze the surface morphology of ITO thin film, providing comprehensive imaging of the structures' size, shape, and distribution. For elemental analysis, Energy-Dispersive X-ray spectroscopy (EDX) was used, which allowed for the identification and quantification of indium, tin, and oxygen within the thin film. The crystal structure of the ITO thin film was investigated using XRD Philips X'Pert Pro Model PW3040 diffractometer equipped with Cu-Kα radiation emitted by copper with the wavelength of 1.5418 Å, which provided details on their crystalline phases and crystallite sizes. The crystallite size (D) was determined using Debye-Scherrer as in Eq. (1):

$$D = \frac{0.9\lambda}{\beta \cos\theta} \tag{1}$$

where λ is X-ray wavelength (1.5406 Å), β is Full Width at Half Maximum (FWHM) of XRD peak in radian and θ is XRD peak position, one half of 2θ. Moreover, lattice strain (ε) was determined using tangent as in Eq. (2):

$$\varepsilon = \frac{\beta}{4 \tan\theta} \tag{2}$$

RESULTS AND DISCUSSIONS

At 1000 °C, low temperature deposition creates small structures with a diameter of around 0.39 μm, as shown in Figure 1(a). SEM analysis revealed small, well-defined structures that are mostly isolated, with minimal agglomeration or coalescence. At this temperature, restricted thermal energy prevents considerable particle growth and interaction, resulting in smooth surfaces and homogenous forms [15,16]. According to Jamnig *et al.* [16], at low temperatures, the limited thermal energy restricts atomic-scale diffusion, thereby reducing adatom mobility. This restriction hinders adatom mobility, leading to smaller grain sizes and less coalescence, resulting in smoother and more homogeneous films. However, while aggregation is significantly reduced under these conditions, it is not entirely absent. According to Jiang *et al.* [17], factors such as insufficient dispersion of precursor materials or ineffective surfactants may cause localized particle clustering. Nevertheless, the total amount of the aggregation remains constrained due to the restricted particle interaction under this temperature.

As the temperature increases to 1100 °C, the structure offers an ideal blend of particle size, structural regularity, and elemental distribution. SEM analysis shows structures with well-defined shape, moderate growth, and limited agglomeration, resulting in a diameter of approximately 0.46 μm, as shown in Figure 1(b). Agglomeration behavior at this temperature is minimized, which enhances both compositional consistency and morphological uniformity in the deposited films. Particle interactions and thermal energy are key factors influencing agglomerate stability during growth [18,19]. The moderate temperature supports controlled adatom mobility and surface diffusion, enabling a more organized microstructure with limited aggregation. Structures synthesized at 1100 °C exhibit better structural morphology as it reduces the negative effects of aggregation while sustaining homogeneity.

Further increasing the deposition temperature to 1200 °C results in substantial aggregation, agglomeration, and coalescence, leading to irregular morphologies and dense clusters with a diameter of approximately 0.58 μm, as shown in Figure 1(c). Excessive thermal energy enhances atomic mobility, resulting in significant particle growth and advanced Ostwald ripening dominates the growth process, causing smaller particles to dissolve

and contribute to the creation of non-uniform structures.

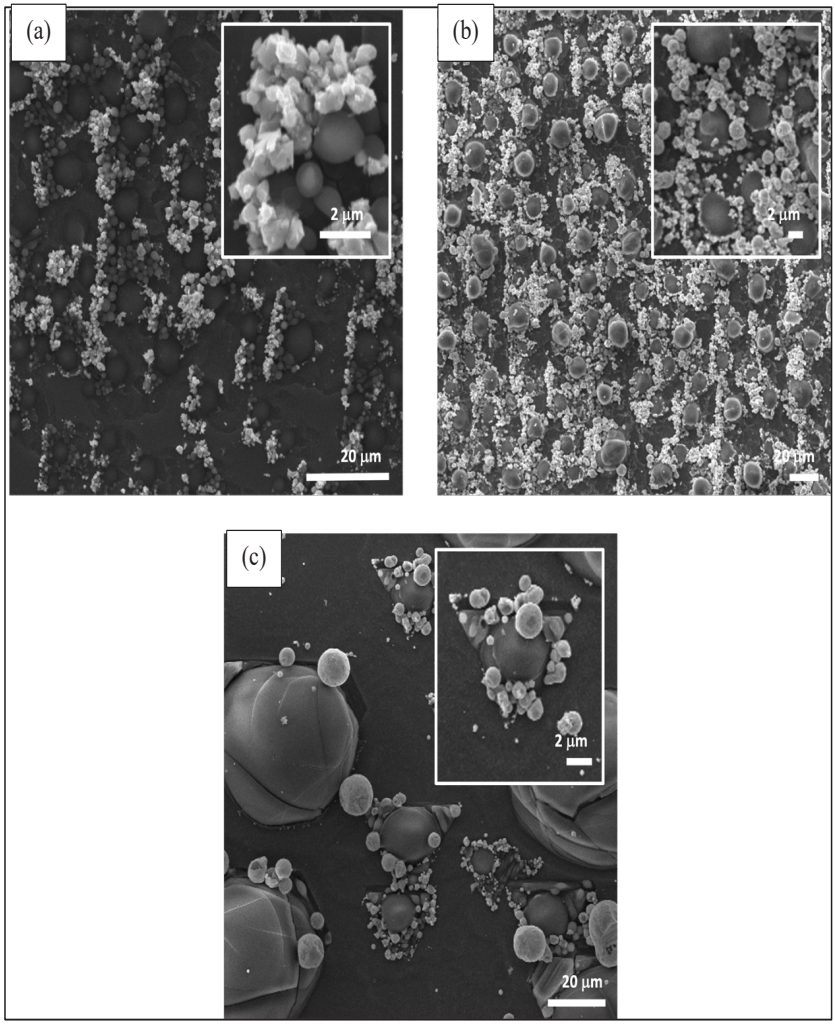

Figure 1: SEM images of the growth of ITO thin film by CVD at varying deposition temperatures of (a-c) 1000, 1100 and 1200 °C, with insets of high magnification images.

The Ostwald ripening mechanism takes place in solid or liquid settings, where small nanoparticles dissolve into monomers and subsequently redeposit onto bigger nanoparticles over time [20]. As the solubility of gases in solids diminishes with increasing temperature, so does the equilibrium concentration, restricting growth through Ostwald ripening [21]. Based on the structural morphology findings, the behavior of aggregated nanoparticles under various deposition temperature emphasizes the need of reaching the right thermal energy during deposition. This connection illustrates that the deposition temperature has an influence not only on the physical properties of ITO structures, but also on the interaction dynamics of particles. Therefore, 1200 °C is an extremely high deposition temperature at which the synthesis process becomes difficult to control, highlighting the need to optimize the deposition temperatures for producing excellent ITO thin films.

The self-catalytic ITO process, which involves the Vapor Solid Liquid (VLS) mechanism, is a well-studied method for producing high-quality nanostructures. A technique for condensing vaporized precursor materials like SnO_2 and In_2O_3 onto catalytic indium-tin alloy droplets produced during synthesis was proposed in [4]. These liquid droplets act as self-catalysts, allowing material to diffuse from the vapor phase into the droplet. As the droplet becomes supersaturated, ITO structures precipitate and develop from its base, generating well-defined one-dimensional structures. The process takes place within a tube furnace, which provides the high temperature required for vaporization, catalytic droplet production, and thin film development. Carbothermal reduction of precursors in the presence of carbon creates metal vapors, which are carried to the substrate by carrier gases for deposition.

Energy-dispersive X-ray spectroscopy (EDX), integrated with SEM, provides a thorough approach to analyze the elemental composition and distribution inside ITO thin film synthesized at various deposition temperatures. EDX confirms the success of the synthesis process by determining the presence of indium (In), tin (Sn), and oxygen (O) in the appropriate stoichiometric ratios. The elemental analysis, as shown in Figure 2 (a-c), validates the inclusion of these components into the structure.

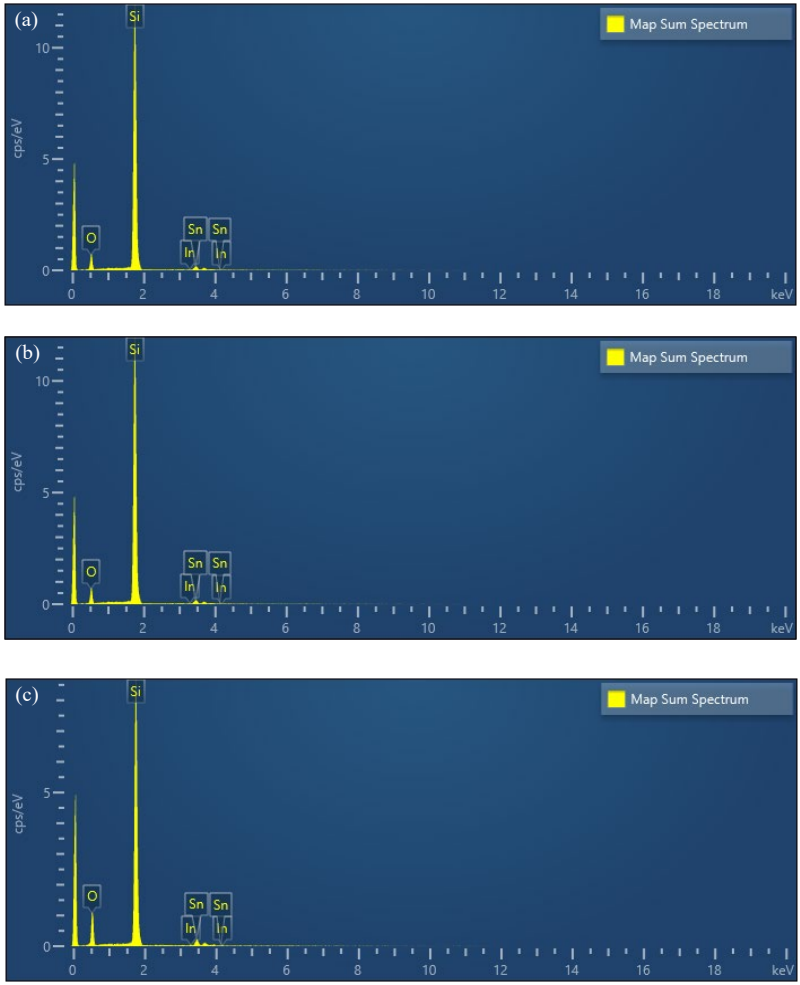

Figure 2: EDX spectrum of ITO thin film at various deposition temperatures (a-c) 1000, 1100 and 1200 °C.

As temperature increase, the EDX analysis reveals distinct compositional trends suggest an early stage of film nucleation at 1000 °C with limited incorporation of metal species. This may be attributed to reduced surface diffusion and lower reactivity at this temperature, which restricts effective precursor decomposition and atomic mobility [16]. At 1100 °C, a significant increase in all elements; O (31.03 at.%), Sn (24.39 at.%), and In (1.04 at.%) indicates enhanced precursor decomposition and

surface diffusion. This temperature appears optimal for promoting the growth of well-formed ITO thin film with higher Sn and In incorporation, resulting in a more complete oxide matrix formation. At 1200 °C, although the In content continues to slightly increase (1.16 at.%), both Sn (10.81 at.%) and O (25.07 at.%) contents decrease compared to 1100 °C. This may be due to thermal desorption or re-evaporation of volatile species at elevated temperatures. Additionally, higher temperatures might alter the kinetics of growth, leading to partial decomposition or non-stoichiometric incorporation of elements [8, 16, 22]. The combination of SEM and EDX gives precise insights into how deposition temperature affects both the structural and compositional properties of the ITO thin film.

Figure 3 shows the XRD patterns of ITO thin film synthesized at different deposition temperatures. The structure consists of orthorhombic SnO, rhombohedral In_2O_3, and cubic $In_2Sn_2O_7$ phases. Peaks of orthorhombic SnO are found at 2θ values of 26.0°, 28.8°, 32.4°, 38.4°, and 78.2°, indicating the crystallographic planes (110), (112), (021), (202), and (208), respectively [JCPDS card No. 01-077-2296]. Additionally, a peak at $2\theta = 65.0°$ is attributed to the (208) plane of rhombohedral In_2O_3 [JCPDS card No. 01-072-0683] and a peak at $2\theta = 31.1°$ corresponds to the (320) plane of cubic $In_2Sn_2O_7$ [JCPDS card No. 00-039-1058] remains present throughout all samples.

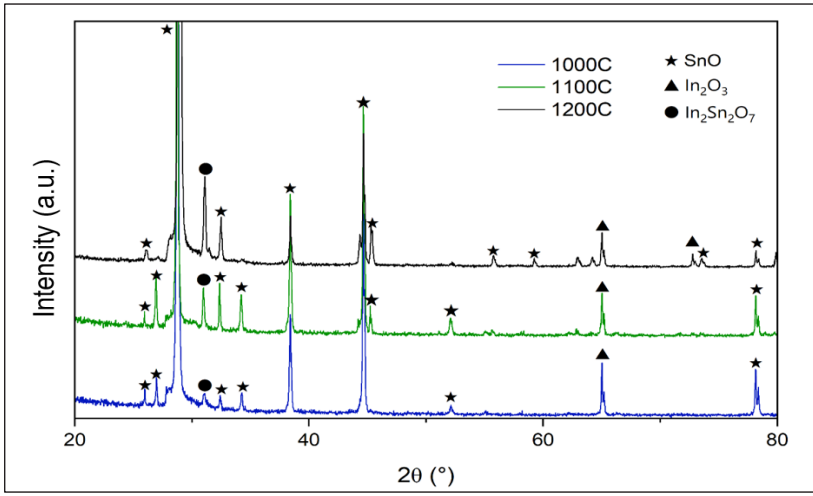

Figure 3: XRD patterns of ITO thin film synthesized at different deposition temperatures.

The XRD patterns of the samples produced at 1100 °C and 1200 °C change noticeably. A new peak of orthorhombic SnO at 45.2° rises which corresponds to the (021) crystallographic plane. Furthermore, at 1200°C, the peaks of orthorhombic SnO at 26.9°, 32.4°, and 44.6°, associated with the (111), (021), and (024) crystallographic planes, have diminished. Meanwhile, new peaks of orthorhombic SnO which appear at 55.8°, 59.2°, and 73.5°, corresponding to the (116), (224), and (136) planes, suggesting changes in phase composition. A new peak at 72.8° of rhombohedral In_2O_3, corresponding to the (312) crystallographic plane, suggesting the growth of In_2O_3 with increasing deposition temperatures. The change in crystal orientation with deposition temperature is attributed to variations in adatom mobility and thermodynamic driving forces. Aforementioned earlier, higher temperatures might alter the kinetics of growth, allow reorganization into more thermodynamically stable orientations [22]. Disappearance or emergence of certain planes reflects thin film evolution and preferred orientation changes at different growth conditions. For calculating the crystallite size and lattice strain of the sample using Eq. (1) and (2), respectively, the peak at $2\theta = 31.1°$, which corresponds to the (320) plane of $In_2Sn_2O_7$ was analyzed. The FWHM, crystallite size and lattice strain are tabulated in Table 1.

Table 1: FWHM, crystallite size, D (nm) and lattice strain (ε) of ITO thin film at various deposition temperatures 1000, 1100 and 1200 °C.

Deposition Temperature (°C)	FWHM (°)	Crystallite Size, D (nm)	Lattice Strain, ε (x 10^{-3})
1000	0.2448	35.17	3.84
1100	0.1224	70.32	1.93
1200	0.0836	102.93	1.31

As temperature increases, the crystallite size increased by 35.17 nm, 70.32 nm, and 102.93 nm for 1000 °C, 1100 °C, and 1200 °C, respectively. Lattice strain decreased correspondingly, with values of 3.84 x 10^{-3}, 1.93 x 10^{-3}, and 1.31 x 10^{-3}, indicating enhanced crystallinity at higher temperatures. The examinations revealed that the size of the crystallite increased with the higher deposition temperature. Moreover, a decrease in FWHM of the peaks can be defined by the increase in crystallite size with temperature, indicating that more growth of the crystallite size is associated with a decrease of peak width [23]. The calculated lattice strain values for the samples decrease with an increase of deposition temperature. According to Ghamari et al. [23], this trend in lattice strain is associated with an increase in peak intensity and a decrease in peak width, which result in increased crystallite sizes and enhanced crystallinity. It is obvious that during the deposition of ITO thin film, the microstructure of a film has a significant impact on the evolution and development of the inherent stress. The Volmer-Weber mode of film growth states that adatom attachment to surface areas at the grain boundaries and grain growth during deposition (at homologous temperatures) compete with one another in the stress evolution [24,25].

CONCLUSION

The self-catalyzed growth of ITO thin film is achieved using CVD technique with varying deposition temperatures. SEM analysis shows that the average diameter of the thin film is 0.39 μm, 0.46 μm, and 0.58 μm for temperatures of 1000 °C, 1100 °C, and 1200 °C, respectively. At 1100 °C, the deposition temperature offers the best conditions for synthesizing indium tin oxide (ITO). SEM analysis reveals the thin film with well-defined shapes, moderate growth, and minimal aggregation. ITO synthesized at 1100 °C exhibit better structural morphology as they reduce the negative effects of aggregation

while sustaining homogeneity, as EDX validated the even distribution of indium, tin, and oxygen, with the greatest homogeneity of 56.46% observed at this temperature. Additionally, the XRD pattern confirms the presence of cubic $In_2Sn_2O_7$ across all samples at $2\theta = 31.1°$ corresponds to the (320) plane. Overall, as the deposition temperature increases, well-defined structures are formed. The average diameter and crystallite size of the thin film also increase, while the lattice strain decreases indicating enhanced crystallinity. In summary, this study analyzes and explains the dependence of structural properties, lattice strain and crystallite size in the development of self-catalyzed ITO structures under different deposition temperatures. To further advance this work, future studies could focus on the electrical and optical performance of these ITO films for the selective optoelectronic device application.

ACKNOWLEDGEMENTS

This work was funded by the Ministry of Higher Education, Malaysia under Fundamental Research Grant Scheme 2021 (FRGS/1/2021/ STG05/ UITM/02/8).

REFERENCES

[1] M. R. Akanda, A. M. Osman, M. K. Nazal & M. A. Aziz, 2020. Review-Recent Advancements in the Utilization of Indium Tin Oxide (ITO) in Electroanalysis without Surface Modification, *Journal of the Electrochemical Society,* 167(3), 037534.

[2] S. M. Yang, H. K. Yen & K. C. Lu, 2022. Synthesis and Characterization of Indium Tin Oxide Nanowires with Surface Modification of Silver Nanoparticles by Electrochemical Method, *Nanomaterials*, 12(6), 897.

[3] M. Stoian, T. Maurer, S. Lamri & I. Fechete, 2021. Techniques of Preparation of Thin Films: Catalytic Combustion, *Catalysts*, 11(12), 1530.

[4] J. Jung & D. H. Kim, 2020. Growth Evolution of Self-catalytic Tin-doped Indium Oxide Nanowires, *Journal of Alloys and Compounds,* 823, 153648 - 153648.

[5] D. Bokov, A. T. Jalil, S. Chupradit, W. Suksatan, M. J. Ansari, I. H. Shewael, G. H. Valiev & E. Kianfar, 2021. Nanomaterial by Sol-Gel Method: Synthesis and Application, *Advances in Materials Science and Engineering*, 2021, 1 - 21.

[6] F. Menchini, L. Serenelli, L. Martini, G. Stracci, E. Salza & M. Tucci, 2025. High Mobility Tungsten-doped Indium Oxide (IWO) Deposited by Room-temperature RF Sputtering in Pure Argon Plasma, *Materials Science in Semiconductor Processing*, 185, 108780.

[7] Y. Cui, S. Zhao, X. Xie, J. Liu & H. Shi, 2022. Preparation of Indium Tin Oxide Nanowires by Using Physical-Vapor-Transport Method, *Journal of Physics: Conference Series*, 2254(1), 012023.

[8] H. Zeng, T. Takahashi, T. Seki, M. Kanai, G. Zhang, T. Hosomi, K. Nagashima, N. Shibata & T. Yanagida, 2020. Oxygen-induced Reversible Sn-dopant Deactivation Between Indium Tin Oxide and Single-crystalline Oxide Nanowire Leading to Interfacial Switching, *ACS Applied Materials & Interfaces*, 12(47), 52929 - 52936.

[9] S. Dhar, S. Mandal, G. Das, W. Li, S. Mukherjee, C. Banerjee, H. Saha & A. K. Barua, 2024. Synthesis of Sputtered Self-catalytic Indium Tin Oxide Nanorods for Photovoltaic Application, *Journal of Alloys and Compounds,* 1004, 175757.

[10] J. Kim, S. Shrestha, M. Souri, J. Connell, S. Park & A. Seo, 2020. High-temperature Optical Properties of Indium Tin Oxide Thin-Films, *Scientific Reports*, 10(1) 12486.

[11] R. K. Sharme, M. Quijada, M. Terrones & M. M. Rana, 2024. Thin Conducting Films: Preparation Methods, Optical and Electrical Properties, and Emerging Trends, Challenges, and Opportunities, *Materials*, 17(18), 4559.

[12] H. D. S. e Silva, F. R. Marciano, A. S. de Menezes, T. H. de Carvalho Costa, L. S. de Almeida, L. S. Rossino, I.O. Nascimento, R.R. M. de Sousa & B. C. Viana, 2020. Morphological Analysis of the TiN Thin film Deposited by CCPN Technique, *Journal of Materials Research and Technology,* 9(6), 13945 - 13955.

[13] L. R. Nivedita, A. Haubert, A.K. Battu & C. V. Ramana, 2020. Correlation Between Crystal Structure, Surface/interface Microstructure, and Electrical Properties of Nanocrystalline Niobium Thin Films, *Nanomaterials*, 10(7), 1287.

[14] W. Kern, 1970. Cleaning Solutions Based on Hydrogen Peroxide for use in Silicon Semiconductor Technology, *RCA Review,* 31(2), 187 - 206.

[15] V. Karoutsos, N. Florini, N. C. Diamantopoulos, C. Balourda, G. P. Dimitrakopulos, N. Bouropoulos & P. Poulopoulos, 2024. On the effect of Randomly Oriented Grain Growth on the Structure of Aluminum Thin Films Deposited via Magnetron Sputtering, *Coatings*, 14(11), 1441.

[16] A. Jamnig, D. G. Sangiovanni, G. Abadias & K. Sarakinos, 2019. Atomic-Scale Diffusion Rates During Growth of Thin Metal Films on Weakly-Interacting Substrates, *Scientific Reports*, 9, 6640.

[17] Z. Jiang, T. Liu, X. Zhai & J. Liu, 2021. Optimization Preparation of Indium Tin Oxide Nanoparticles via Microemulsion Method using Orthogonal Experiment, *Crystals,* 11(11), 1387.

[18] E. S. Golomako, V.I. Saverchenko & S.P. Fisenko, 2024. Deposition of Nanoparticles and Their Agglomerates from a Laminar Gas Flow onto a Substrate, *Journal of Engineering Physics and Thermophysics,* 97, 1820 - 1824.

[19] Y. Yu, J. K. Madhukesh, U. Khan, A. Zaib, A. H. Abdel-Aty, I. S. Yahia, M. S. Alqahtani, F. Wang & A. M. Galal, 2022. Nanoparticle Aggregation and Thermophoretic Particle Deposition Process in the

Flow of Micropolar Nanofluid Over a Stretching Sheet, *Nanomaterials,* 12(6), 977 - 977.

[20] H. Ye, Z. Zhang & R. Wang, 2023. Nucleation and Growth of Nanocrystals Investigated by In Situ Transmission Electron Microscopy, *Small,* 19(49), 2303872.

[21] S. H. B. Teo, M. A. Thompson, M. Bilokur, D. Bhattacharyya & C. S. Corr, 2024. Investigating the Temperature Dependence of Helium Bubble Dynamics in Plasma Exposed Tungsten via In-Situ TEM Annealing, *Materialia*, 35, 102110 - 102110.

[22] N. M. Ahmed, F. A. Sabah, H. I. Abdulgafour, A. Alsadig, A. Sulieman & M. Alkhoaryef, 2019. The Effect of Post Annealing Temperature on Grain Size of Indium-Tin-Oxide for Optical and Electrical Properties Improvement, *Results in Physics*, 13, 102159.

[23] F. Ghamari, D. Raoufi & J. Arjomandi, 2021. Influence of Thickness on Crystallographic, Stereometric, Optoelectronic, and Electrochemical Characteristics of Electron-Beam Deposited Indium Tin Oxide Thin Films, *Materials Chemistry and Physics,* 260, 124051-124051.

[24] A. S. Pashchenko, O. V. Devitsky, L. S. Lunin, M. L. Lunina, O. S. Pashchenko & E. M. Danilina, 2023. Growth of Nanotextured Thin Films of GaInAsP and GaInAsSbBi Solid Solutions on GaP Substrates by Pulsed Laser Deposition, *Nanosystems: Physics, Chemistry, Mathematics*,14(5), 601 - 605.

[25] N. Zhao, S. Wu, Y. Wang, F. Liu, Y. Ma, H. Zhang, M. Liu & Y. Zheng, 2022. Fabrication of Gold-Based “Sphere-on-Plate” Hybrid Nanostructures with Dual Plasmonic Absorptions Covering Visible and Near-Infrared II Windows via the Volmer–Weber Growth Mode, *Langmuir,* 38(31), 9669 - 9677.